Available online at www.sciencedirect.com
SCIENCE DIRECT®
Computers and Chemical Engineering 27 (2003) 1185–1199
Computers & Chemical Engineering
www.elsevier.com/locate/compchemeng

Dynamic modeling and control of yeast cell populations in continuous biochemical reactors

Michael A. Henson *

Department of Chemical Engineering, University of Massachusetts, Amherst, MA 01003-9303, USA

Received 6 February 2003; accepted 7 February 2003

Abstract

Biochemical reactors are essential unit operations in a wide variety of biotechnological processes. As compared to conventional chemical reactors, bioreactors present unique modeling and control challenges due to the complexity of the underlying biochemical reactions and the heterogenous nature of cell populations. The dynamic behavior of bioreactors can be strongly affected by variations between individual cells that are captured only with cell population models. This paper is intended to highlight our recent work on dynamic modeling and feedback control of yeast cell populations in continuous bioreactors. The results presented demonstrate the feasibility of using cell population models as the basis for dynamic analysis and model-based control of continuous yeast bioreactors. The paper concludes with a short discussion of future research needs in this challenging area.

Keywords: Biochemical reactors; Yeast cultures; Cell population modeling; Bifurcation analysis; Model-based control

1. Introduction

The goal of biochemical engineering research is industrial production of biologically based products such as foods and beverages, pharmaceuticals and various commodity and specialty chemicals. The biochemical manufacturing industry is growing rapidly due to dramatic advancements in biotechnology and the high value of biochemical products such as pharmaceuticals (Lee, 1992). Process control has played a limited role in the biochemical industry because the economic incentives for improved process operation often are dwarfed by costs associated with product research and development. This situation is expected to change due to the expiration of key patents and the continuing development of global competition. Another obstruction to process control has been the lack of on-line sensors for key process variables. While this will remain an issue for the foreseeable future, recent advancements in biochemical measurement technology make the development of advanced process control systems a realistic goal.

A continuous biochemical reactor (also known as a continuous fermentor) used to grow microbial cells is depicted in Fig. 1. Medium is supplied continuously to the reactor to sustain growth of the cell population. The medium contains substrates metabolized by the cells during growth as well as other constituents such as mineral and salts required to mimic the natural growth environment. The agitator speed is chosen to provide sufficient mixing while avoiding excessive shear forces that may damage the cells (Lee, 1992). A stream is removed continuously from the reactor to achieve constant volume operation. The removal rate is characterized by the dilution rate, which is the reciprocal of the reactor residence time. The effluent stream contains unreacted substrates, cellular biomass and various metabolites produced by the cells. Desired products may be the cells themselves and/or some combination of the metabolites. Off-gases such as carbon dioxide also are produced as byproducts of the biochemical reactions.

Mathematical modeling of microbial cell growth kinetics continues to be an important focus of biochemical engineering research (Nielsen and Villadsen, 1994).

* Tel.: +1-413-545-3481; fax: +1-413-545-1647.
E-mail address: henson@ecs.umass.edu (M.A. Henson).

0098-1354/03/$ - see front matter © 2003 Elsevier Science Ltd. All rights reserved.
doi:10.1016/S0098-1354(03)00046-2

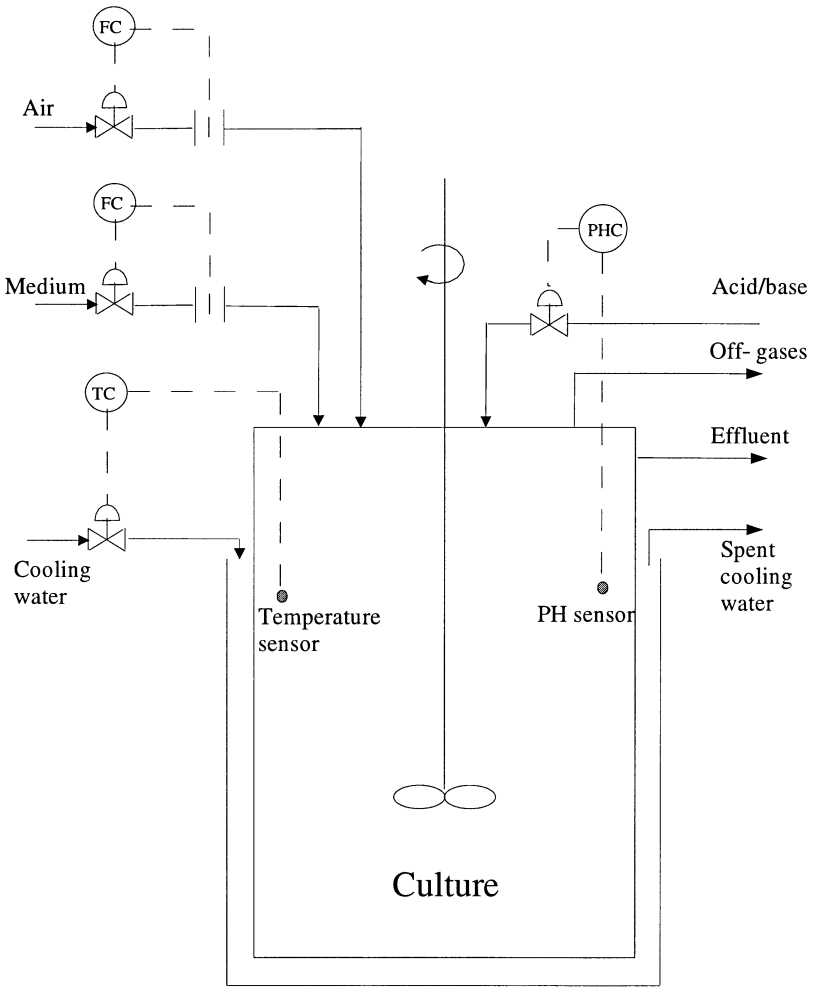

Fig. 1. Continuous biochemical reactor.

The potential impact of predictive models on bioprocess simulation, design, optimization and control is substantial. As compared to conventional chemical reactors, bioreactors are particularly difficult to model due to the complexity of the biochemical reactions, the unique characteristics of individual cells and the lack of key process measurements. The consumption of substrates and production of metabolites result from hundreds of coupled biochemical reactions (Mauch, Arnold, and Reuss, 1997). Construction and dynamic modeling of these complex reaction networks is a very challenging problem. While they often are viewed as homogeneous mixture of identical cells, microbial cultures actually are comprised of heterogeneous mixtures of cells that differ with regard to size, mass and intracellular concentrations of proteins, DNA and other chemical constituents (Srienc and Dien, 1992). Accurate modeling of cell growth and metabolite formation kinetics may require that individual cells be differentiated based on these characteristics.

As shown in Fig. 1, a typical control system for a continuous bioreactor consists of simple feedback loops that regulate reactor liquid volume, temperature and pH. The control system is designed to supply a constant nutrient flow that is expected to maximize steady-state cell growth in the absence of external disturbances. This open-loop control strategy does not ensure satisfactory regulation of key output variables such as the biomass and product concentrations. The development of closed-loop control strategies for direct biomass/metabolite optimization would represent a significant advance in the biochemical industry. Such control strategies require the availability of appropriate dynamic models and on-line measurements of key process variables. These technical obstructions and the lack of clear economic incentives have hindered the implementation of model-based control systems on industrial bioreactors. Recent progress in bioreactor modeling and measurement techniques and the increasing realization that improved bioreactor operation is necessary to remain competitive has motivated new research on cell population modeling, dynamics and control.

The objective of this paper is to highlight our recent work on dynamic modeling and control of continuous

yeast bioreactors described by cell population models. In Section 2, a yeast cell population model that includes a simple structured description of the extracellular environment is presented. Section 3 contains dynamic simulation and bifurcation analysis results for the yeast model. The potential impact of recent advances in cell distribution measurement technology on the development of model-based control strategies is illustrated in Section 4 where simulation results for a model predictive controller that allows direct control of yeast cell distribution properties are presented. Section 5 contains a short discussion of future research needs in cell population modeling and control.

2. Yeast cell population modeling

2.1. Background

Saccharomyces cerevisiae (baker's yeast) is an important microorganism in the brewing, baking, food manufacturing and genetic engineering industries. Baker's yeast can be produced in continuous bioreactors by supplying a nutrient stream containing the substrate glucose. As shown in Fig. 2, yeast cells proliferate via an asymmetric process known as budding (Hjortso and Nielsen, 1994). A daughter cell grows until it reaches a critical mass called the transient mass (m_t^*). At this point the cell is called a mother cell. All further growth occurs in the bud attached to the mother cell. At a critical mass called the division mass (m_d^*) the mother cell and the bud divide to produce a newborn daughter cell and a newborn mother cell.

Many investigators have shown that continuous yeast bioreactors can exhibit complex dynamic behavior characterized by the unpredictable appearance and disappearance of sustained oscillations (Parulekar, Semones, Rolf, Lievense, and Lim, 1986; Strassle, Sonnleitner, and Fiechter, 1989; von Meyenburg, 1973).

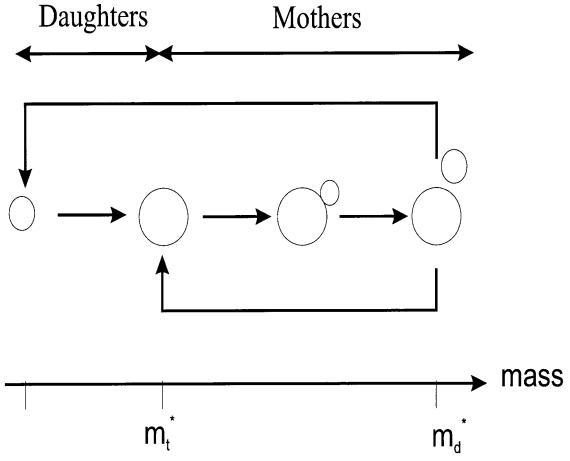

Fig. 2. Simplified cell cycle for budding yeast.

While the asymmetric cell cycle has been hypothesized to play a key role, the underlying cellular mechanisms that cause oscillatory yeast dynamics are controversial. Understanding and manipulating these dynamics could lead to important advances in yeast production processes and provide key insights into the cellular behavior of more complex cells present in higher organisms.

Our group has been developing a cell population model based on the simple description of the asymmetric yeast cell cycle to rationalize the oscillatory dynamics observed experimentally. The long-term goal is to design model-based controllers that improve bioreactor operability and productivity through the attenuation and/or stabilization of the oscillatory open-loop dynamics. A key feature of the cell population model is that the transition and division masses vary with the glucose concentration in the extracellular environment. Our previously published model (Zhu, Zamamiri, Henson, and Hjortso, 2000) is unstructured in the sense that other constituents of the extracellular environment are neglected completely. This unstructured model lacks variables that can be compared directly to readily available extracellular measurements such as the dissolved oxygen and evolved carbon dioxide concentrations. Below our recently developed cell population model (Mhaskar, Henson, and Hjortso, 2002) which contains a simple structured description of the extracellular environment is presented. Although not discussed here for the sake of brevity, the model structure is well suited for the application of estimation techniques aimed at determining unknown parameters from experimental data (Mhaskar, Henson, and Hjortso, 2002).

2.2. Model formulation

The population balance equation (PBE) that describes the evolution of the cell mass number distribution is formulated as follows (Eakman, Fredrickson, and Tsuchiya, 1996):

$$\frac{\partial W(m,t)}{\partial t} + \frac{\partial [K(S')W(m,t)]}{\partial m} = \int_0^{m'} 2p(m,m')\Gamma(m',S')W(m',t)\mathrm{d}m' - [D+\Gamma(m)]W(m,t) \quad (1)$$

where m is the cell mass; $W(m,t)$ is the cell number density; $K(S')$ is the overall single cell growth rate; S' is the effective substrate concentration (defined below); $p(m,m')$ is the newborn cell probability function; $\Gamma(m,S')$ is the division intensity function; and D is the dilution rate. The division intensity function is modeled as:

$$\Gamma(m,S') = \begin{cases} 0 & m \le m_t^* + m_o \\ \gamma e^{-\varepsilon(m-m_d^*)^2} & m \in [m_t^* + m_o, m_d^*] \\ \gamma & m \ge m_d^* \end{cases} \quad (2)$$

where m_t^* and m_d^* are the cell transition and division masses, respectively; m_o is the additional mass beyond m_t^* that mother cells must gain before division is possible; and ε and γ are constant parameters. This function models the probabilistic nature of cell division. The newborn cell probability function has the form:

$$p(m,m') = A\exp[-\beta(m-m_t^*)^2] + A\exp[-\beta(m-m'+m_t^*)^2] \quad (3)$$

when $m < m'$ and $m' > m_t^* + m_o$; the function is identically zero otherwise. Here A and β are constant parameters. This function yields two Gaussian peaks in the cell number distribution, one centered at m_t^* corresponding to mother cells and one centered at $m_t^* - m'$ corresponding to daughter cells.

Yeast cell cycle events are affected by the extracellular environment through a highly complex set of signaling processes. In principle, these relationships can be captured by a structured bioreactor model (Nielsen and Villadsen, 1994). We pursue a much simpler approach that preserves the unstructured nature of the intracellular description. The transition and division masses are assumed to be functions of the effective substrate concentration:

$$m_t^*(S') = \begin{cases} m_{t0} + K_t(S_l - S_h) & S' < S_l \\ m_{t0} + K_t(S' - S_h) & S' \in [S_l, S_h] \\ m_{t0} & S' > S_h \end{cases} \quad (4)$$

$$m_d^*(S') = \begin{cases} m_{d0} + K_d(S_l - S_h) & S' < S_l \\ m_{d0} + K_d(S' - S_h) & S' \in [S_l, S_h] \\ m_{d0} & S' > S_h \end{cases} \quad (5)$$

where S_l, S_h, m_{t0}, m_{d0}, K_t and K_d are constants. These saturation functions are consistent with experimental observations that the ratio of the division and transition masses increases as the nutrient concentration increases (Alberghina, Ranzi, Porro, and Martegani, 1991).

The following reaction sequence accounts for the major metabolic pathways (glucose fermentation, glucose oxidation and ethanol oxidation) thought to be involved in oscillatory yeast dynamics:

$$C_6H_{12}O_6 \rightarrow 2C_2H_5OH + 2CO_2$$

$$C_6H_{12}O_6 + 6O_2 \rightarrow 6CO_2 + 6H_2O$$

$$C_2H_5OH + 3O_2 \rightarrow 2CO_2 + 3H_2O \quad (6)$$

The glucose fermentation rate K_{gf} is assumed to follow Monod kinetics with respect to glucose. The glucose oxidation rate K_{go} and the ethanol oxidation rate K_{eo} are assumed to follow Monod kinetics with respect to the associated substrate and dissolved oxygen. Preferential consumption of glucose as compared to ethanol is modeled by introducing a glucose inhibition term in the ethanol oxidation rate. The resulting rate expressions are:

$$K_{gf}(G') = \frac{\mu_{mgf} G'}{K_{mgf} + G'} \quad (7)$$

$$K_{go}(G',O) = \frac{\mu_{mgo} G'}{K_{mgo} + G'} \frac{O}{K_{mgd} + O} \quad (8)$$

$$K_{eo}(G',E',O) = \frac{\mu_{meo} E'}{K_{meo} + E'} \frac{O}{K_{med} + O} \frac{K_{inhib}}{K_{inhib} + G'} \quad (9)$$

where O is the dissolved oxygen concentration; μ_{mgf}, μ_{mgo} and μ_{meo} are maximum consumption rates; K_{mgf}, K_{mgo}, K_{mgd}, K_{meo} and K_{med} are saturation constants; and K_{inhib} is a constant that characterizes the inhibitory effect of glucose on ethanol fermentation. The overall single cell growth rate $K(S')$ is the sum of the growth rates due to the three metabolic pathways.

The substrate mass balance equations are:

$$\frac{dG}{dt} = D(G_f - G) - \int_0^\infty \left[\frac{K_{gf}(G')}{Y_{gf}} + \frac{K_{go}(G')}{Y_{go}}\right] W(m,t)dm \quad (10)$$

$$\frac{dE}{dt} = D(E_f - E) + \frac{92}{180}\int_0^\infty f(m)\frac{K_{gf}(G')}{Y_{gf}} W(m,t)dm - \int_0^\infty \frac{K_{eo}(E')}{Y_{eo}} W(m,t)dm \quad (11)$$

where G and E are the glucose and ethanol concentrations, respectively; G' and E' are the effective glucose and ethanol concentrations, respectively; G_f and E_f are the feed glucose and ethanol concentrations, respectively; Y_{gf}, Y_{go} and Y_{eo} are constant yield coefficients; and the ratio 92/180 represents the mass of ethanol produced per mass of glucose fermentatively consumed. Experimental data suggests that ethanol is excreted primarily by budded cells (Alberghina, Ranzi, Porro, and Martegani, 1991). The function $f(m)$ in Eq. (11) is used to model this behavior:

$$f(m) = \begin{cases} 0 & m \le m_t^* \\ \gamma_e \exp[-\varepsilon_e(m - m_t^* - m_e)^2] & m > m_t^* \end{cases} \quad (12)$$

where γ_e, ε_e and m_e are constant parameters. The filtered substrate concentrations model the delayed response of cell metabolism to changes in the extracellular environment:

$$\frac{dG'}{dt} = \alpha_g(G - G') \quad (13)$$

$$\frac{dE'}{dt} = \alpha_e(E - E') \quad (14)$$

where α_g and α_e are constants.

The liquid phase oxygen balance is written as:

$$\frac{dO}{dt} = K_{lo}a(O^* - O) - \int_0^\infty \left[\frac{192}{180}\frac{K_{go}(G')}{Y_{go}} + \frac{96}{46}\frac{K_{eo}(E')}{Y_{eo}}\right] W(m,t)dm \quad (15)$$

where O^* is the saturation oxygen concentration; K_{lo} is the oxygen mass transfer coefficient; a is the interfacial area per unit liquid volume; the ratio 192/180 represents the mass of oxygen consumed per mass of glucose oxidatively metabolized; and the ratio 96/46 represents the mass of oxygen consumed per mass of ethanol metabolized. The oxygen solubility is assumed to be governed by Henry's law:

$$O^* = H_O RTO_{out} \quad (16)$$

where H_O is the Henry's rate constant for oxygen; O_{out} is oxygen partial pressure in the gas exhaust stream; T is the absolute temperature; and R is the gas constant. The gas phase oxygen balance is:

$$\frac{dV_g O_{out}}{dt} = F(O_{in} - O_{out}) - K_{lo}a(O^* - O)V_l \quad (17)$$

where V_g and V_l are the gas phase and liquid phase volumes, respectively; F is the volumetric air feed flow rate; and O_{in} is the oxygen partial pressure in the air feed stream.

The liquid phase carbon dioxide balance is:

$$\frac{dC}{dt} = K_{lc}a(C^* - C) + \int_0^\infty \left[\frac{264}{180}\frac{K_{go}(G')}{Y_{go}} + \frac{88}{46}\frac{K_{eo}(E')}{Y_{eo}}\right] W(m,t)dm + \int_0^\infty \left[f(m)\frac{88}{180}\frac{K_{gf}(G')}{Y_{gf}}\right] W(m,t)dm \quad (18)$$

where C is the liquid phase carbon dioxide concentration; C^* is the saturation carbon dioxide concentration; K_{lc} is the carbon dioxide mass transfer coefficient; the ratio 264/180 represents the mass of carbon dioxide produced per mass of glucose oxidatively metabolized; the ratio 88/46 represents the mass of carbon dioxide produced per mass of ethanol metabolized; and the ratio 88/180 represents the mass of carbon dioxide produced per mass of glucose fermentatively metabolized. The carbon dioxide solubility is modeled as:

$$C^* = H_C(\text{pH})RTC_{out} \quad (19)$$

where H_C is the Henry's constant for carbon dioxide which is evaluated at a pH of 5.0; and C_{out} is the carbon dioxide partial pressure in the exhaust gas stream. The gas phase carbon dioxide balance is:

$$\frac{dV_g C_{out}}{dt} = F(C_{in} - C_{out}) - K_{lc}a(C^* - C)V_l \quad (20)$$

where C_{in} is the carbon dioxide partial pressure in the air feed stream.

The yeast cell population model contains approximately 40 parameters which must be specified. Values for parameters such as yield coefficients and maximum growth rates available in the literature are listed in Table 1. Also listed in this table are nominal operating conditions used in our laboratory experiments. Other parameter such as constants in the division intensity and newborn probability functions are not available. The parameter values listed in Table 2 have been chosen to obtain qualitative agreement with experimental data. Although not discussed here, a limited number of these parameters can be estimated from data to improve the predictive capability of the model (Mhaskar, Henson, and Hjortso, 2002).

3. Yeast cell population dynamics

3.1. Experimental data

Many investigators have shown that continuous yeast bioreactors can exhibit sustained oscillations that are reflected in measurements of intracellular and extracellular variables (Parulekar, Semones, Rolf, Lievense, and Lim, 1986; Strassle, Sonnleitner, and Fiechter, 1989; von Meyenburg, 1973). Sustained oscillations are observed only for a specific range of dilution rates (Parulekar, Semones, Rolf, Lievense, and Lim, 1986); stable steady-states are obtained for dilution rates below and above this range. In collaboration with Prof. Martin Hjortso (LSU), laboratory experiments were undertaken to further explore this dynamic phenomenon. Batch and continuous culture experiments were performed using a Bioflo 3000 fermenter (New Brunswick) with a working

Table 1
Experimentally derived cell population model parameters

Variable	Value	Variable	Value
Y_{gf}	0.15 g/g	μ_{mgf}	30×10^{-13} g/h
Y_{go}	0.65 g/g	μ_{mgo}	3.25×10^{-13} g/h
Y_{eo}	0.5 g/g	μ_{meo}	7×10^{-13} g/h
K_{mgf}	40 g/l	K_{mgo}	2 g/l
K_{meo}	1.3 g/l	K_{inhib}	0.4 g/l
K_{mgd}	0.001 g/l	K_{med}	0.001 g/l
H_O	0.0404 g/l/atm	H_C	1.48 g/l/atm
V_g	0.9 l	V_l	0.1 l
$K_l a$	1500 h^{-1}	$K_l c$	1500 h^{-1}
D	0.15 h^{-1}	G_f	30 g/l
E_f	0 g/l	F	90 l/h
T	298 K	O_{in}	0.21 atm
C_{in}	0.0003 atm		

Table 2
Other cell population model parameters

Variable	Value	Variable	Value
γ	400	ε	7
γ_e	8	ε_e	20
m_o	1×10^{-13} g	m_e	1.54×10^{-13} g
A	$\sqrt{10/\pi}$	β	40
S_l	0.1 g/l	S_h	2.0 g/l
K_t	0.01 g/g l	K_d	3.83 g/g l
m_{to}	4.55×10^{-13} g	m_{do}	10.25×10^{-13} g
α_g	20	α_e	20

volume of 1.0 l. The fermenter was interfaced to a personal computer with the necessary software for data collection and basic regulatory control functions. Details on medium preparation and the experimental protocol are available elsewhere (Zamamiri, Birol and Hjortso, 2001).

The top plot in Fig. 3 shows the dynamic response obtained for batch startup followed by a switch to continuous operation. The exhaust gas CO_2 concentration is used as a representative output variable for the culture. Following inoculation with yeast cells at $t = 0$, the bioreactor was operated in batch mode to allow a sufficient density of cells to be produced. Sustained oscillations were observed immediately following the switch to continuous operation at $t = 20$ h. The lower plot in Fig. 3 shows the cell number distribution as a function of cell size at the times indicated in the top plot. Two distinct cell subpopulations were formed as the culture progresses through batch growth. The first and second peaks represent subpopulations of daughter cells and mother cells, respectively. As discussed below, the presence of such well defined subpopulations is strongly correlated to the subsequent appearance of sustained oscillations.

Another experiment was designed to test our hypothesis that a stable steady state and a periodic attractor can exist at the same operating conditions. A representative set of results is shown in Fig. 4 (Zamamiri, Birol, and Hjortso, 2001). The experiment started with oscillatory dynamics that were obtained by switching the

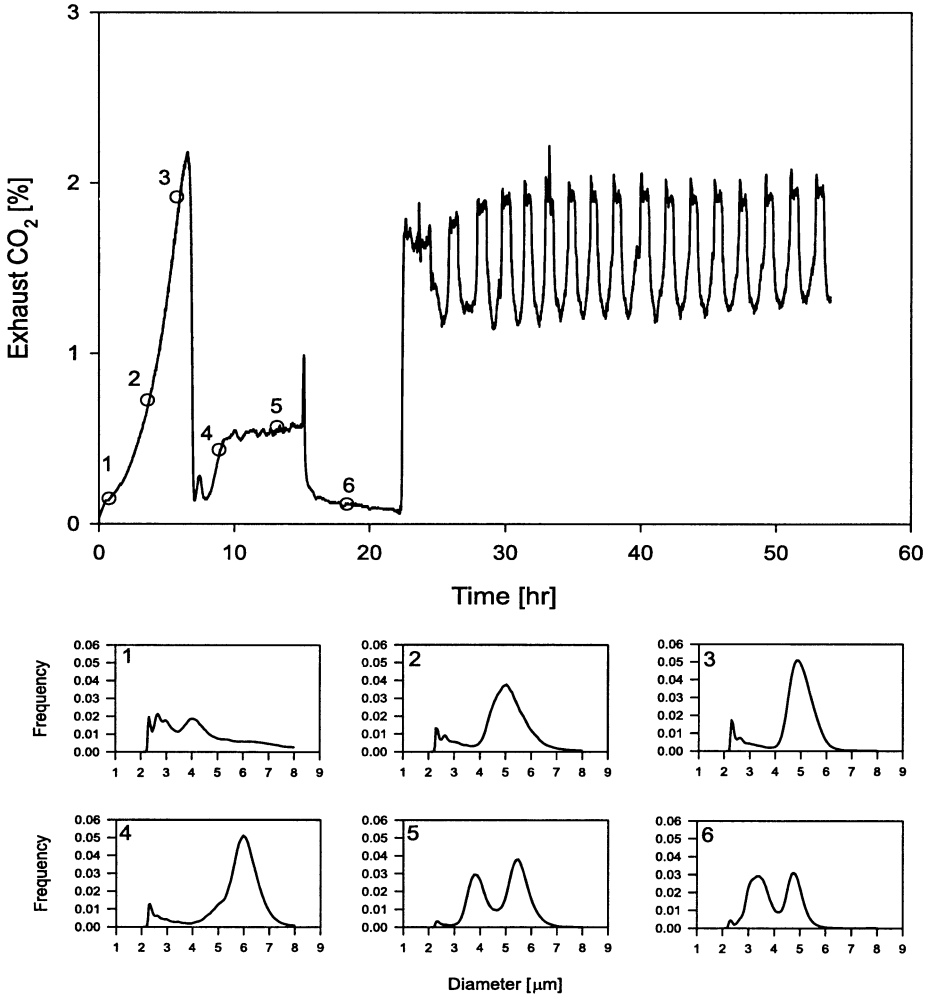

Fig. 3. Experimental switch from batch to continuous operation.

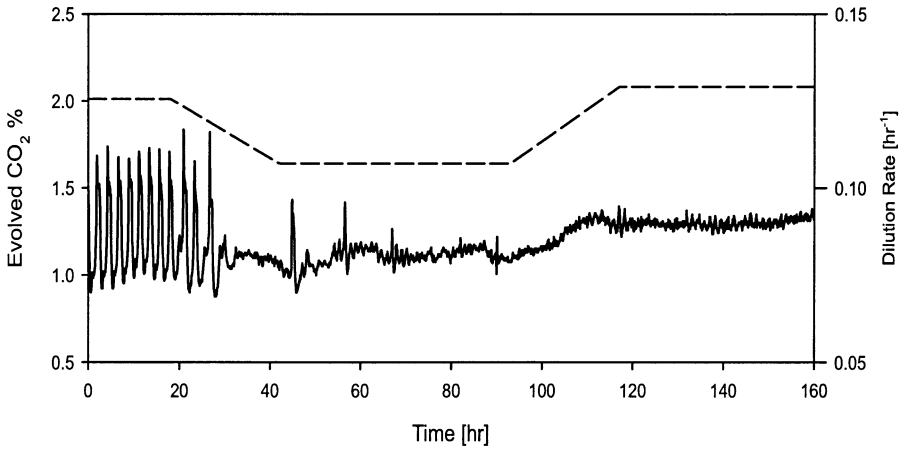

Fig. 4. Experimental ramp changes in dilution rate (Zamamiri, Birol and Hjortso, 2001).

culture from batch to continuous operation. Starting at $t = 20$ h, the dilution rate was slowly ramped down over a 24-h period until oscillations disappear. The stationary state was preserved for two days with the dilution rate maintained at this low value. Starting at $t = 92$ h, the dilution rate was slowly ramped up at the same rate as used for the negative ramp. No significant oscillations were observed even though the steady-state dilution rate produced oscillations at the beginning of the experiment. This strongly suggests the existence of multiple attractors at the same dilution rate.

While lumped parameter models have been proposed (Cazzador, 1991; Jones and Kompala, 1999), we believe that cell population models have the best potential for rationalizing the complex dynamic behavior observed in continuous yeast bioreactors. Several investigators (Munch, Sonnleitner, and Fiechter, 1992; Strassle, Sonnleitner, and Fiechter, 1989) have shown that the appearance of sustained oscillations is related to the formation of distinct cell subpopulations via a mechanism known as cell cycle synchrony. As shown in Fig. 3, a synchronized culture is characterized by well defined peaks in the cell number distribution that correspond to cell subpopulations which collectively pass through the cell cycle. Cell cycle synchrony establishes a direct relationship between the cell population and oscillatory dynamics. Experimental data suggests that sustained oscillations occur only if the cell population is sufficiently organized into distinct subpopulations. Otherwise, dispersive effects inherent in the heterogeneous cell population overwhelms the synchronization effect and result in a stable steady state. This provides a physical explanation for the existence of multiple attractors at the same operating conditions as shown in Fig. 4.

3.2. Dynamic simulation results

The cell population model presented in Section 2 is comprised of a coupled set of nonlinear algebraic, integro-ordinary differential and integro-partial differential equations. We have found that orthogonal collocation on finite elements (Finlayson, 1980) provides efficient and robust model solution. A finite cell mass domain, $0 \leq m \leq m_{\max}$, is chosen such that the number of cells with mass $m > m_{\max}$ is effectively zero. The population balance equation is approximated by a coupled set of nonlinear ordinary differential equations obtained by discretizing the mass domain. Integral expressions in the population and substrate balance equations are approximated using Gaussian quadrature (Finlayson, 1980). Solution stability is not strongly affected by the number of finite elements and collocation points. A converged solution is obtained with twelve equally spaced finite elements, each with eight internal collocation points that are determined as the roots of the appropriate Jacobi polynomial (Finlayson, 1980). These parameters are used in the subsequent simulations, resulting in 109 total collocation points. The state vector of the discretized cell population model consists of the cell number density at each collocation point as well as the eight extracellular concentrations. Therefore, the discretized model consists of 117 nonlinear ordinary differential equations.

A comparison between model predictions and experimental data for batch startup followed by a switch to continuous operation at $t = 20$ h is shown in Fig. 5. The two peaks observed experimentally during batch growth represent increased carbon dioxide production due to oxidative consumption of glucose and ethanol (first peak) and fermentative consumption of glucose (second peak). The model predicts the oxidative growth phase reasonably well, but the fermentative growth phase is not captured adequately. Following the switch to continuous operation, the model produces sustained oscillations with amplitude and period in good agreement with experimental data. In both cases, the transition to sustained oscillations is very rapid.

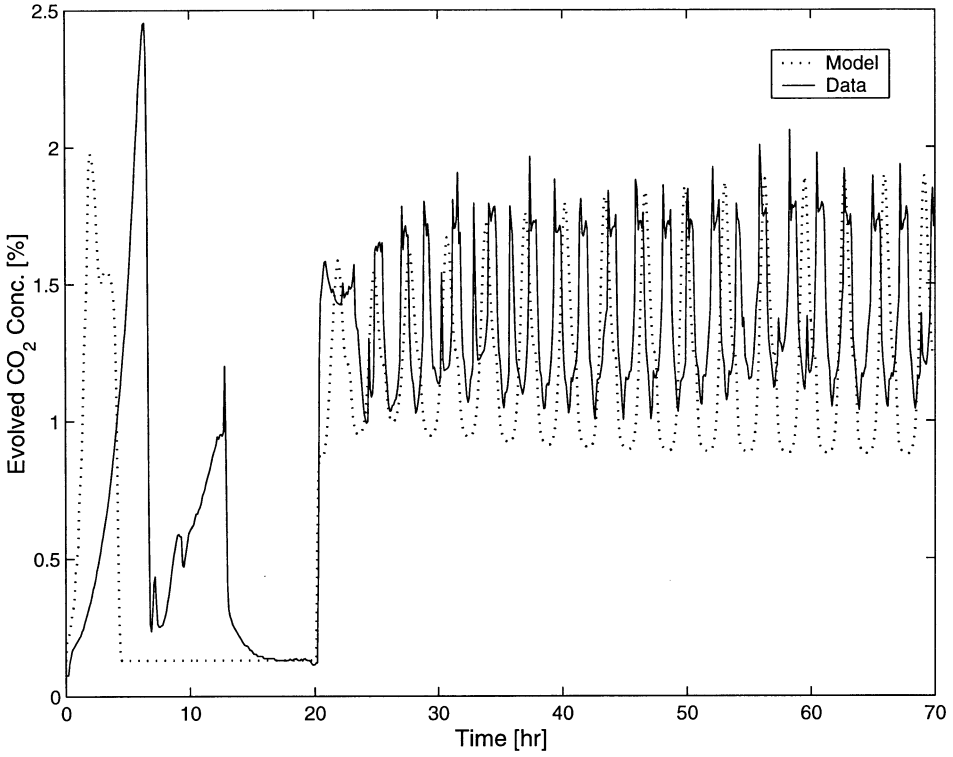

Fig. 5. Comparison of model and experiment for switch from batch to continuous operation.

Model and experimental responses for ramp changes in the dilution rate are shown in Fig. 6. The series of dilution rate changes are identical to those used to produce the experimental data in Fig. 4. The predicted oscillations at the beginning of the test are very similar to those observed experimentally. Following the nega-

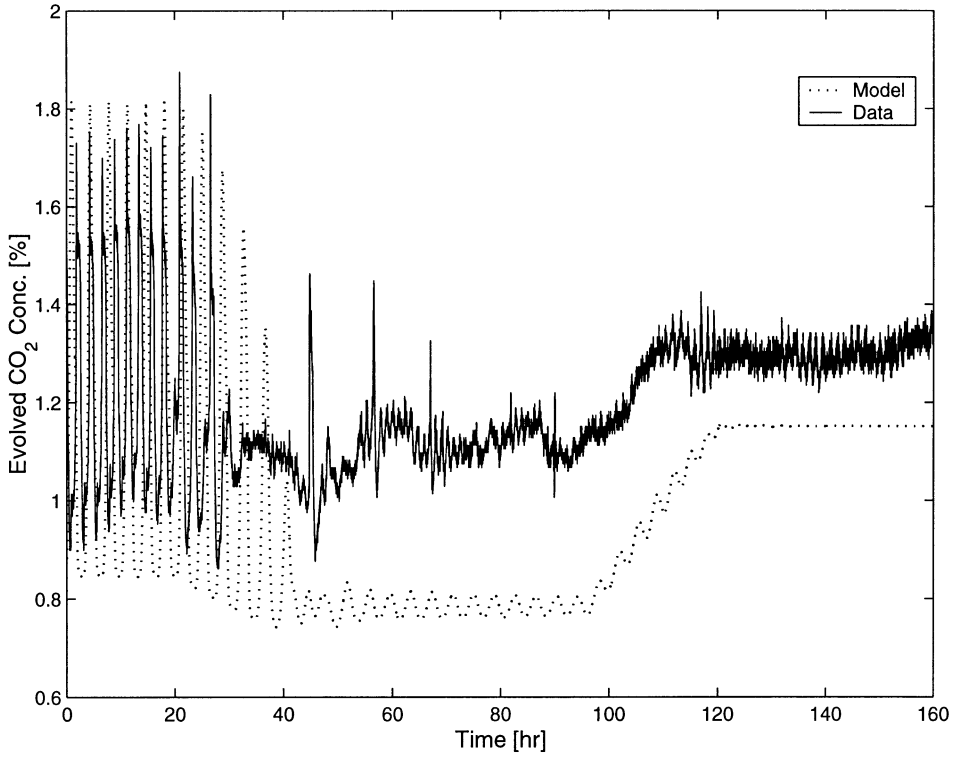

Fig. 6. Comparison of model and experiment for ramp changes in dilution rate.

tive ramp change, the model predicts that oscillations will be strongly attenuated but not completely eliminated. This prediction is consistent with experimental data because the small amplitude oscillations predicted by the model are below the noise level in the carbon dioxide measurement. Following the positive ramp change, the model predicts that oscillations will disappear completely. This test demonstrates that the model structure is capable of supporting multiple attractors at the same operating conditions as observed experimentally.

The effect of the initial cell number distribution on the model response is illustrated in Figs. 7 and 8. An initial distribution that leads to a stable steady-state solution is shown in the top plot of Fig. 7. As shown in the bottom plot, the initial distribution is sufficiently disorganized for the oscillations to slowly decay. The final distribution shown in the top plot is very dispersed as compared to the initial distribution. A slightly more organized initial distribution that leads to sustained oscillations is shown in the top plot of Fig. 8. The oscillation amplitude grows until a stable periodic solution is obtained. Two well defined peaks that correspond to daughter and mother cell subpopulations are present in the final distribution. These tests verify that the model is consistent with experimental observations that sustained oscillations are intimately related to cell cycle synchrony and the formation of distinct cell subpopulations. Given their similarities, the initial distributions shown in Figs. 7 and 8 appear to be near the separatix that divides the domains of attraction of the two solutions.

3.3. Bifurcation analysis results

In our previous publications (Zhang and Henson, 2001; Zhang, Zamamiri, Henson, and Hjortso, 2002), we have argued that bifurcation analysis allows more insightful comparisons of bioreactor model predictions and experimental data than is possible with dynamic simulation alone. Such analysis can be applied to the yeast cell population model to characterize the bifurcations that result in appearance and disappearance of periodic solutions. Because bifurcation theory has been developed primarily for nonlinear ordinary differential equation systems (Kuznetsov, 1995), the discretized version of the cell population model is utilized for analysis.

The first task is to determine local stability of steady-state solutions. This is achieved by computing the eigenvalues of the Jacobian matrix evaluated at each steady-state of interest. A dilution rate where one or more eigenvalues cross the imaginary axis is known as a bifurcation point. Locating periodic solutions and determining their stability is a more difficult problem. We utilize a continuation code specifically designed for high-dimensional systems obtained from Prof. Yannis

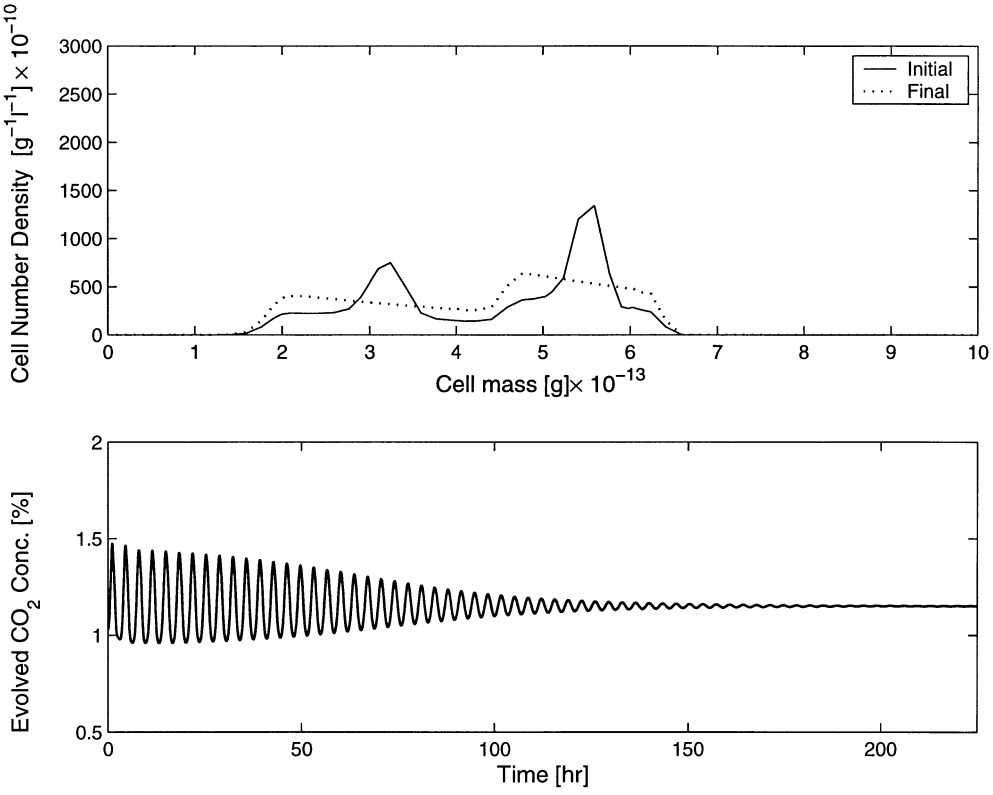

Fig. 7. Model prediction of steady state.

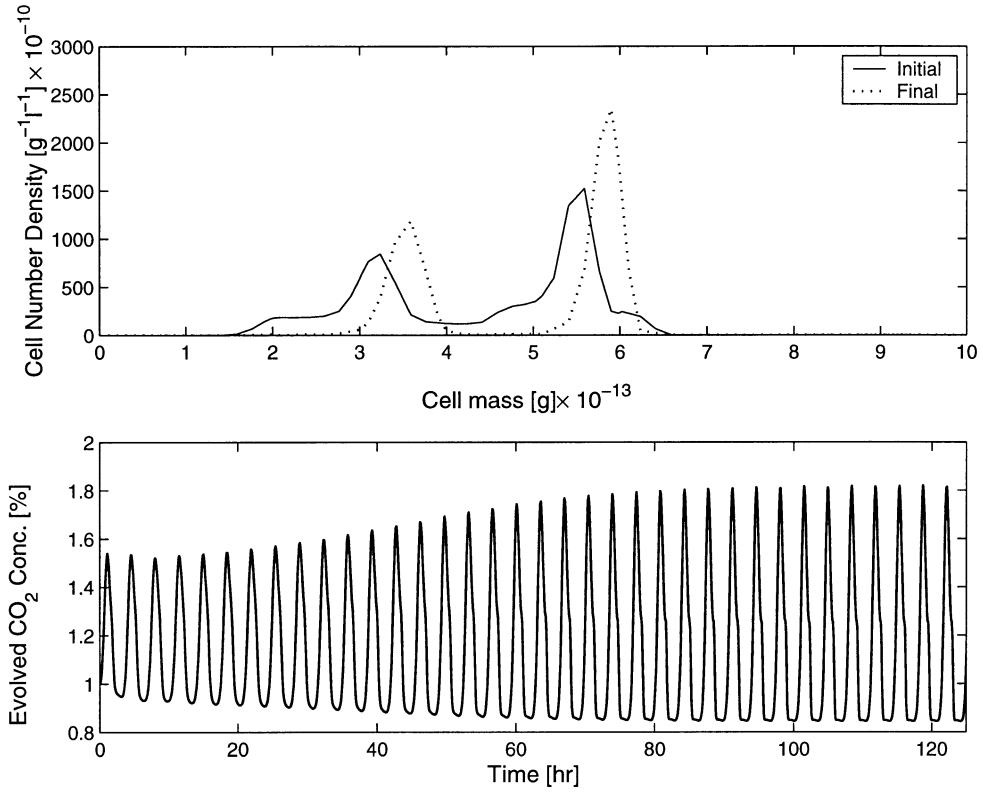

Fig. 8. Model prediction of sustained oscillations.

Kevrekidis (Princeton) (Krishnan, Baer, and Imbihl, 2000). A good initial guess of the state variables and the oscillation period corresponding to the limit cycle must be supplied to achieve convergence. For stable periodic solutions, the initial guess is obtained readily by dynamic simulation.

A bifurcation diagram for the discretized cell population model is shown in Fig. 9 where the dilution rate (D) is the bifurcation parameter and the glucose concentration (S) is chosen as a representative output variable. The model possesses a single stable steady-state solution (+) at low dilution rates. As the dilution rate is increased, a bifurcation occurs where the steady-state solution becomes unstable (○) and a stable periodic solution with oscillations of the amplitude indicated (– – –) appears. This subcritical Hopf bifurcation is accompanied by the appearance of large amplitude oscillations. The stable periodic solution exists with the unstable steady-state solution for a large range of dilution rates. As the dilution rate is increased further, a second bifurcation occurs where the periodic solution disappears and the steady-state solution regains its stability. This subcritical Hopf bifurcation is characterized by small amplitude oscillations. There is a small range of dilution rates near the subcritical bifurcation that supports both steady-state and periodic attractors. The domains of attractions of the two asymptotic solutions are separated by an unstable periodic solution with oscillations of the amplitude indicated (—). This result provides a simple qualitative explanation for the dynamic simulation results presented above.

4. Yeast cell population control

4.1. Motivation

Feedback control is necessary to ensure satisfactory performance of continuous yeast bioreactors in the presence of external disturbances and/or changes in operational requirements. As depicted in Fig. 1, a typical bioreactor control system consists of simple regulatory loops designed to maintain environmental conditions that promote cell growth. Such schemes do not allow direct control of variables such as biomass and metabolite concentrations that determine profitability of the bioprocess. During the last decade, substantial work has been focused on the development of more advanced adaptive and/or nonlinear control strategies for continuous bioreactors (Bastin and Dochain, 1990; Hoo and Kantor, 1986; Kurtz, Henson, and Hjortso, 2000). These methods are based on lumped parameter models that neglect the heterogeneous nature of the cell population.

Lack of suitable on-line measurements has been a major obstruction to the development of controller design techniques based on cell population models.

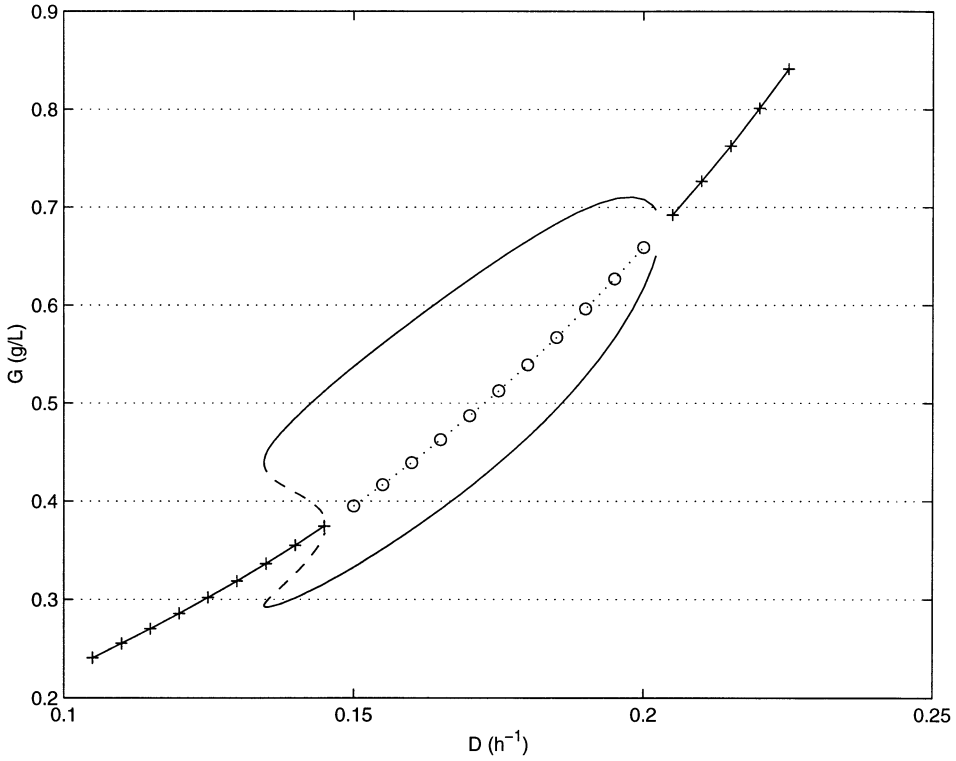

Fig. 9. Bifurcation diagram for cell population model.

This barrier is less daunting with the development of biochemical measurement technology such as flow cytometry which enables cell distribution properties to be elucidated. Flow cytometry allows individual cells to be differentiated with respect to their protein content, DNA content and other intracellular properties (Alberghina, Ranzi, Porro, and Martegani, 1991; Srienc, 1999). Recently, flow cytometry has been combined with flow injection systems that allow on-line measurement of cell distribution properties (Zhao, Natarajan, and Srienc, 1999). This provides motivation for the development of advanced control strategies in which cell population models are utilized to manipulate cell cycle characteristics and/or regulate cell property distributions.

Our work on continuous yeast bioreactor control has been focused on modifying the open-loop dynamics that result in sustained oscillations (Zhang, Zamamiri, Henson, and Hjortso, 2002; Zhu, Zamamiri, Henson, and Hjortso, 2000). A possible control objective is stabilization of a particular steady state to eliminate oscillations that adversely affect bioreactor stability and productivity. In some situations, the induction and stabilization of oscillations that lead to increased production of key metabolites synthesized only during part of the cell cycle my be desirable (Hjortso, 1996). Below a linear model predictive control (LMPC) strategy which allows either control objective to be achieved is presented. The cell population model used for controller design is a simplified version of the model presented in Section 2 where the extracellular environment is described by the concentration of a single rate limiting substrate. Additional details are available in the original reference (Zhu, Zamamiri, Henson, and Hjortso, 2000).

4.2. Model predictive control strategy

A linear controller design model is generated directly from the discretized cell population model. The nonlinear model equations are linearized about the steady-state operating point and temporally discretized with sampling time $\Delta t = 0.1$ h. The resulting state-space model has the form:

$$x(k+1) = Ax(k) + Bu(k)$$

$$y(k) = Cx(k) \tag{21}$$

where $x \in R^{111}$ is the state vector comprised of the cell mass number density at each collocation point (W_j) and the substrate and effective substrate concentrations (S, S'); $u \in R^2$ is the input vector comprised of the dilution rate (D) and the feed substrate concentration (S_f); and $y \in R^m$ is the output vector defined below. The cell mass number distribution is assumed to be measured via a method such as flow cytometry. The controllability matrix for the pair (A, B) has rank four due to the large state dimension and the strong collinearity of the state variables. This indicates that the cell distribution

cannot be modified arbitrarily with the two input variables available.

The controller design model is completed by defining the controlled output vector. A straightforward approach is to choose the cell number density at each collocation point as a controlled output. This can be problematic because: (i) the control problem is highly non-square (2 inputs, 109 outputs); (ii) cell number densities at nearby collocation points are strongly collinear; and (iii) the substrate concentration also needs to be controlled to avoid washout. We have found that good closed-loop performance can be achieved by controlling a subset of the cell number densities and the substrate concentration:

$$y = [W_{j_1} \quad W_{j_2} \quad \cdots W_{j_p} \quad S]^T \tag{22}$$

where the indices $\{j_1, \ldots, j_p\}$ define the collocation points where the associated cell number density is used as a controlled output. In the subsequent simulations, the controlled cell number densities are chosen to be the boundary points of the finite elements. The output vector of Eq. (22) results in a much lower dimensional problem (14 outputs) than the full-order case.

The LMPC controller is formulated as (Muske and Rawlings, 1993):

$$\begin{aligned}\min_{U_N(k)} \sum_{j=0}^{\infty} \{&[y(k+j|k) - y_s]^T Q[y(k+j|k) - y_s] \\ &+ [u(k+j|k) - u_s]^T R[u(k+j|k) - u_s] \\ &+ \Delta u^T(k+j|k) S \Delta u(k+j|k)\}\end{aligned} \tag{23}$$

where $y(k+j|k)$ and $u(k+j|k)$ are predicted values of the output and input vectors, respectively; y_s and u_s are target values for the output and input vectors, respectively; and $\Delta u(k) = u(k) - u(k-1)$. The decision variables are current and future values of the inputs: $U_N(k) = [u(k|k) \ldots u(k+N-1|k)]$ where N is the control horizon. The inputs are subject to saturation constraints of the form: $u_{\min} \le u \le u_{\max}$. The infinite horizon problem in Eq. (23) can be reformulated as a finite horizon problem and solved using standard quadratic programming software (Muske and Rawlings, 1993). Only the first calculated input actually is implemented, $u(k) = u(k|k)$, and the problem is resolved at the next time step with new measurements. The target vectors u_s and y_s can be adjusted on-line using a disturbance model to eliminate offset (Muske and Rawlings, 1993). In this application, there is little motivation to utilize a disturbance model because there are insufficient degrees of freedom to drive the entire cell distribution to an arbitrary target distribution.

Fig. 10 shows the ability of the LMPC controller to stabilize a desired steady-state operating point. The initial cell number distribution $W(m, 0)$ is a highly synchronized distribution corresponding to a stable periodic solution, while the setpoint vector is obtained from the discretized cell mass distribution at the desired steady-state operating point. Representative output variables shown are the zeroth-order moment of the cell number distribution $m_0 = \int_0^\infty W(m,t)\mathrm{d}m$ and the substrate concentration (S). The solid line is the LMPC controller response and the dashed line is the open-loop response obtained in the absence of feedback control. LMPC yields rapid attenuation of the open-loop oscillations. Evolution of the cell number distribution is shown in Fig. 11. The initial distribution has two well defined subpopulations that typically produce sustained oscillations. The controller attenuates the oscillations and achieves the desired steady-state distribution by counteracting cell synchrony via dispersion of the subpopulations.

Fig. 12 demonstrates the ability of the LMPC controller to stabilize a desired periodic solution. The initial cell number distribution represents a steady-state solution, while distributions corresponding to the desired periodic solution are defined as a time-varying setpoint trajectory. The controller stabilizes the periodic solution by generating oscillatory input moves. Although not shown here, oscillations with the same period are maintained when the controller is switched off and the bioreactor runs under open-loop conditions. Evolution of the cell mass distribution is shown in Fig. 13. The oscillating dynamics are accompanied by marked synchronization of the cell population. Two distinct subpopulations can be identified after 24 h of operation. These results suggest that feedback control strategies which provide direct control of the cell distribution properties have the potential to enhance the stability and productivity of continuous yeast bioreactors.

5. Future research directions

This paper has provided an overview of our recent work in yeast cell population modeling, dynamics and control. The results presented demonstrate the feasibility of using cell population models as the basis for dynamic analysis and feedback control of continuous yeast bioreactors.

Additional work is required to produce engineering techniques of practical utility. Some possible directions for future research include:

1. Derivation of cell population models with intracellular structure to enhance understanding of the complex interactions between individual cell metabolism and cell population dynamics. The cell ensemble modeling approach (Domach and Shuler, 1984; Henson, Muller, and Reuss, 2002) appears to be particulary promising.

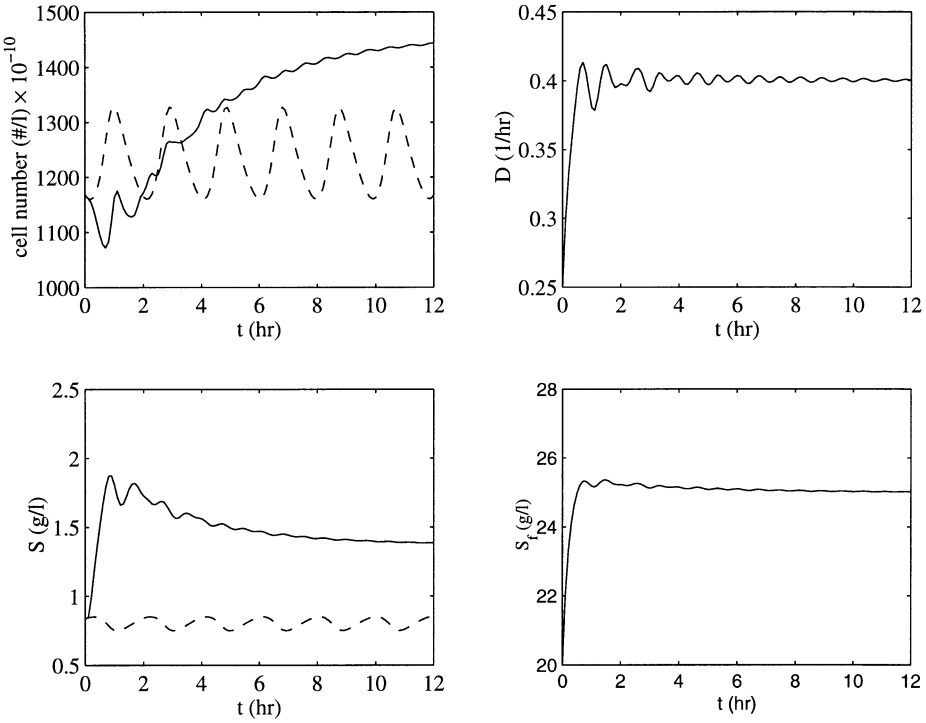

Fig. 10. Feedback stabilization of a steady-state solution.

2. Development of numerical solution and dynamic analysis techniques for structured cell population models. An overview of available solution strategies for cell population models is presented in a recent review paper (Daoutidis and Henson, 2002).

3. Application of parameter estimation techniques to achieve quantitative agreement between cell population model predictions and experimental data. Some initial results are presented in a recent paper (Mhaskar, Henson, and Hjortso, 2002).

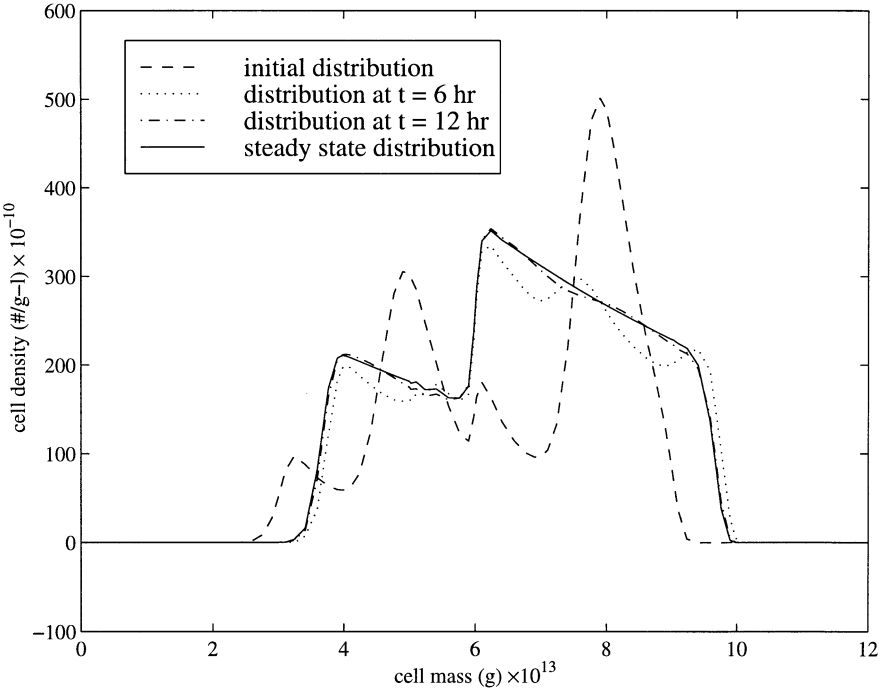

Fig. 11. Cell number distribution evolution for steady-state solution stabilization.

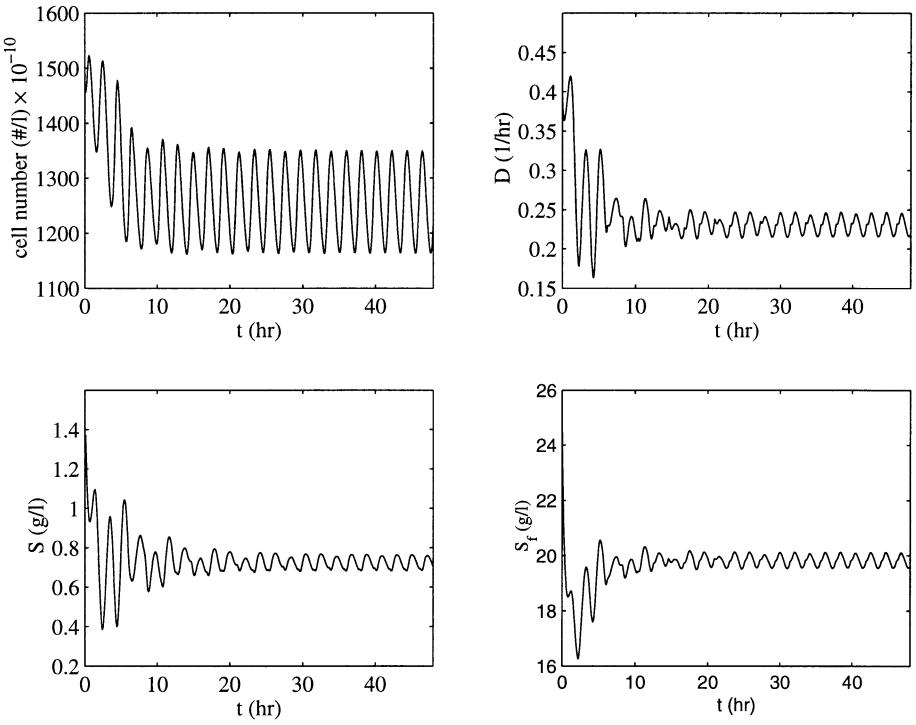

Fig. 12. Feedback stabilization of a periodic solution.

4. Development of cell distribution control strategies that exploit recent advances in biochemical measurement technology such as on-line flow cytometry. The LMPC strategy (Zhu, Zamamiri, Henson and Hjortso, 2000) discussed above is just a first step in this direction.

5. Collection of laboratory data for evaluation and refinement of cell population modeling, dynamics and control techniques. Oscillatory dynamics in yeast cultures (Aon, Cortassa, Westerhoff and van Dam, 1992; Keulers, Satroutdinov, Suzuki and Kuriyama, 1996;

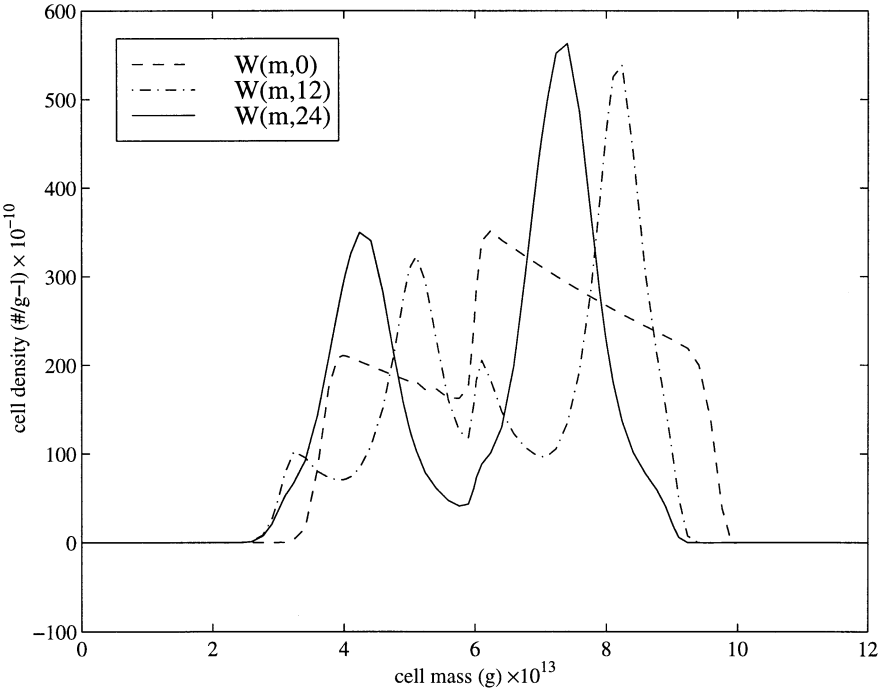

Fig. 13. Cell number distribution evolution for periodic solution stabilization.

Parulekar, Semones, Rolf, Lievense and Lim, 1986) seem well suited for this task.

Acknowledgements

The author would like to acknowledge Prof. Martin Hjortso (LSU), Prof. Yannis Kevrekidis (Princeton) and the former LSU students Dr. Abdelqader Zamamiri, Dr. Guang-Yan Zhu, Dr. Yongchun Zhang and Prashant Mhaskar for their contributions to the research results included in the paper.

References

Alberghina, L., Ranzi, B. M., Porro, D., & Martegani, E. (1991). Flow cytometry and cell cycle kinetics in continuous and fed-batch fermentations of budding yeast. *Biotechnology Progress 7*, 299–304.

Aon, M. A., Cortassa, S., Westerhoff, H. V., & van Dam, K. (1992). Synchrony and mutual stimulation of yeast cells during fast glycolytic oscillations. *Journal of General Microbiology 138*, 2219–2227.

Bastin, G., & Dochain, D. (1990). *On-line estimation and adaptive control of bioreactors*. Amsterdam: Elsevier Science.

Cazzador, L. (1991). Analysis of oscillations in yeast continuous cultures by a new simplified model. *Bulletin of Mathematical Biology 53*, 685–700.

Daoutidis, P., & Henson, M. A. (2002). Dynamics and control of cell populations in continuous bioreactors. *American Institute of Chemical Engineering, Symposium Series 326*, 274–289.

Domach, M. M., & Shuler, M. L. (1984). A finite representation model for an asynchronous culture of *E. coli*. *Biotechnology and Bioengineering 26*, 877–884.

Eakman, J. M., Fredrickson, A. G., & Tsuchiya, H. H. (1996). Statistics and dynamics of microbial cell populations. *Chemical Engineering Progress, Symposium Series 62*, 37–49.

Finlayson, B. A. (1980). *Nonlinear analysis in chemical engineering*. New York: McGraw-Hill.

Henson, M. A., Muller, D., & Reuss, M. (2002). Cell population modeling of yeast glycolytic oscillations. *Biochemical Journal 368*, 433–446.

Hjortso, M. A. (1996). Population balance models of autonomous periodic dynamics in microbial cultures: their use in process optimization. *Canadian Journal of Chemical Engineering 74*, 612–620.

Hjortso, M. A., & Nielsen, J. (1994). A conceptual model of autonomous oscillations in microbial cultures. *Chemical Engineering Science 49*, 1083–1095.

Hoo, K. A., & Kantor, J. C. (1986). Global linearization and control of a mixed-culture bioreactor with competition and external inhibition. *Mathematical Biosciences 82*, 43–62.

Jones, K. D., & Kompala, D. S. (1999). Cybernetic modeling of the growth dynamics of *Saccharomyces cerevisiae* in batch and continuous cultures. *Journal of Biotechnology 71*, 105–131.

Keulers, M., Satroutdinov, A. D., Suzuki, T., & Kuriyama, H. (1996). Synchronization affector of autonomous short-period-sustained oscillation of *Saccharomyces cerevisiae*. *Yeast 12*, 673–682.

Krishnan, J., Baer, M., & Imbihl, R. (2000). Pulse dynamics and interaction on anisotropic surfaces: a computer-assisted study. *Chemical Engineering Science 55*, 257.

Kurtz, M. J., Henson, M. A., & Hjortso, M. A. (2000). Nonlinear control of competitive mixed culture bioreactors via specific cell adhesion. *Canadian Journal of Chemical Engineering 78*, 237–247.

Kuznetsov, Y. A. (1995). *Elements of applied bifurcation theory*. New York: Springer–Verlag.

Lee, J. M. (1992). *Biochemical engineering*. Englewood Cliffs, NJ: Prentice-Hall.

Mauch, K., Arnold, S., & Reuss, M. (1997). Dynamic sensitivity analysis for metabolic systems. *Chemical Engineering Science 52*, 2589–2598.

Mhaskar, P., Henson, M. A., & Hjortso, M. A. (2002). Cell population modeling and parameter estimation of continuous cultures of *Saccharomyces cerevisiae*. *Biotechnology Progress 18*, 1010–1026.

Munch, T., Sonnleitner, B., & Fiechter, A. (1992). New insights into the synchronization mechanism with forced synchronous cultures of *Saccharomyces cerevisiae*. *Journal of Biotechnology 24*, 299–313.

Muske, K. R., & Rawlings, J. B. (1993). Model predictive control with linear models. *American Institute of Chemical Engineering Journal 39*, 262–287.

Nielsen, J., & Villadsen, J. (1994). *Bioreaction engineering principles*. New York: Plenum Press.

Parulekar, S. J., Semones, G. B., Rolf, M. J., Lievense, J. C., & Lim, H. C. (1986). Induction and elimination of oscillations in continuous cultures of *Saccharomyces cerevisiae*. *Biotechnology and Bioengineering 28*, 700–710.

Srienc, F. (1999). Cytometric data as the basis for rigorous models of cell population dynamics. *Journal of Biotechnology 71*, 233–238.

Srienc, F., & Dien, B. S. (1992). *Kinetics of the cell cycle of Saccharomyces cerevisiae. Annuals of the New York Academy of Sciences 665*, 59–71.

Strassle, C., Sonnleitner, B., & Fiechter, A. (1989). A predictive model for the spontaneous synchronization of *Saccharomyces cerevisiae* grown in continuous culture. II. Experimental verification. *Journal of Biotechnology 9*, 191–208.

von Meyenburg, H. K. (1973). Stable synchrony oscillations in continuous culture of *Saccharomyces cerevisiae* under glucose limitation. In B. Chance, E. K. Pye, A. K. Shosh & B. Hess (Eds.), *Biological and biochemical oscillators* (pp. 411–417). New York: Academic Press.

Zamamiri, A. M., Birol, G., & Hjortso, M. A. (2001). Multiple stable states and hysteresis in continuous, oscillating cultures of budding yeast. *Biotechnology and Bioengineering 75*, 305–312.

Zhang, Y., & Henson, M. A. (2001). Bifurcation analysis of continuous biochemical reactor models. *Biotechnology Progress 17*, 647–660.

Zhang, Y., Zamamiri, A. M., Henson, M. A., & Hjortso, M. A. (2002). Cell population models for bifurcation analysis and nonlinear control of continuous yeast bioreactors. *Journal of Process Control 12*, 721–734.

Zhao, R., Natarajan, A., & Srienc, F. (1999). A flow injection flow cytometry system for on-line monitoring of bioreactors. *Biotechnology and Bioengineering 62*, 609–617.

Zhu, G.-Y., Zamamiri, A. M., Henson, M. A., & Hjortso, M. A. (2000). Model predictive control of continuous yeast bioreactors using cell population models. *Chemical Engineering Science 55*, 6155–6167.